

Stochastic cloaking: concealing a region from diffusive particles

Connor Roberts,^{1,*} Ziluo Zhang,^{1,2} Helder Rojas,³ Stefano Bo,⁴
Carlos Escudero,³ Sébastien Guenneau,^{5,†} and Gunnar Pruessner^{1,‡}

¹*Department of Mathematics, Imperial College London, SW7 2AZ, United Kingdom*

²*Wenzhou Institute, University of Chinese Academy of Sciences, Wenzhou, Zhejiang 325001, China*

³*Departamento de Matemáticas Fundamentales Universidad Nacional de Educación a Distancia,
Calle de Juan del Rosal 10, 28040 Madrid, Spain*

⁴*Department of Physics, King's College London, WC2R 2LS, United Kingdom*

⁵*Department of Physics, Imperial College London, SW7 2AZ, United Kingdom*

(Dated: October 8, 2024)

We present a novel class of cloaking in which a region of space is concealed from an ensemble of diffusing particles whose individual trajectories are governed by a stochastic (Langevin) equation. In particular, we simulate how different interpretations of the Langevin equation affect the cloaking performance of an annular single-layer invisibility cloak of smoothly varying diffusivity in two dimensions. Near-perfect cloaking is achieved under the Itô convention, indicated by the cloak preventing particles from accessing an inner core while simultaneously preserving the particle density outside the cloak relative to simulations involving no protected region (and no cloak). Even better cloaking performance can be achieved by regularising the singular behaviour of the cloak—which we demonstrate through two different approaches. These results establish the foundations of “stochastic cloaking”, which we believe to be a significant milestone following that of optical and thermal cloaking.

Introduction — The advent of artificial “metamaterials” has led to the proposal of various exotic phenomena that were once considered the realm of science fiction [1–4]. Notably, by capitalising on the form-invariance of Maxwell’s equations under a coordinate transformation [5], Pendry suggested suitable tuning of the magnetic permeability and electric permittivity of a metamaterial could be used to deviate electromagnetic radiation around an object in such a way that the radiation is undisturbed from its original trajectory [6]. The metamaterial acts as an invisibility cloak in this case, since any observer outside of the metamaterial would be unable to detect the presence of the concealed object and, crucially, the metamaterial itself. This notion of “transformation optics” has inspired research into other forms of radiation from which an object could be cloaked.

A major milestone is that of thermal cloaking, based on the aptly named “transformation thermodynamics” [7–9], where a region of space is protected from changes in its temperature by a surrounding metamaterial of spatially varying thermal conductivity. This demonstrated that transformation-based cloaking is not just restricted to elliptic differential equations—describing optics and acoustics [10, 11]—but is equally applicable to parabolic differential equations. Yet, both are examples of *deterministic* differential equations.

Till now, there has been no equivalent demonstration of cloaking for a system whose constituents are governed by a *stochastic* differential equation, i.e. a system whose random behaviour can be analysed *statistically*, but can

otherwise not be predicted *precisely*. Such a demonstration would be another significant milestone for cloaking, not least because of the inherent difficulties introduced by stochasticity. The major difficulty lies in that the governing stochastic equation—the Langevin equation—is only a “pre-equation” due to being uniquely determined only after choosing a particular discretisation scheme under which to integrate it [12]. This is also known as the Itô vs. Stratonovich dilemma [12–16], named after the first two conventions to be proposed [17, 18]. Even though each convention is at least 60 years old, the fact that they lead to different physical properties of a system is still of great interest today [19].

The corresponding density of a stochastic system evolves according to a Fokker-Planck equation, which is generally not form-invariant under a coordinate transformation. Despite this and the difficulties posed by stochasticity, we demonstrate here—for the first time—that an annular metamaterial of spatially varying diffusivity can be used to cloak an inner core from an ensemble of stochastically diffusing point particles when interpreted under the Itô convention. The properties of the metamaterial, henceforth referred to as “the cloak”, are determined from a coordinate transformation that maps the inner core to the surrounding cloak, as in Fig. 1.

In analogy to optical and thermal cloaking, the cloaking here is signified by particles being unable to access the inner core, as well as a particle density outside the cloak that is agnostic to the region of space being protected. The latter is quantified through a novel proposal to analyse the arrival distribution of particles downstream of the cloak.

Langevin equation — The time evolution of the position $x(t)$ of a single diffusive particle in one dimension is

* connor.roberts16@imperial.ac.uk

† s.guenneau@imperial.ac.uk

‡ g.pruessner@imperial.ac.uk

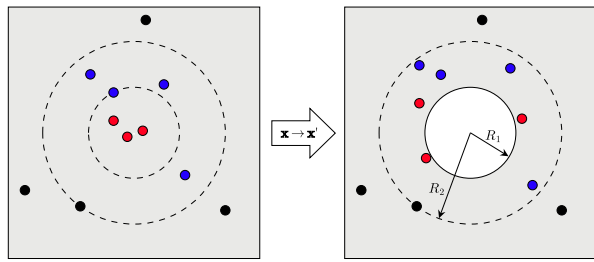


FIG. 1. Schematic representation of a coordinate transformation that tears a hole in the metric space of a two-dimensional plane (left) to produce a finite region, indicated in white, that particles are unable to enter (right). Particle positions at radii $r \geq R_2$ (black points) are invariant under the transformation, while the radii of particles at $r < R_2$ (red and blue points) increase under the transformation.

governed by a stochastic differential (Langevin) equation,

$$\frac{m}{\gamma(x)} \ddot{x}(t) = -\dot{x} + \sqrt{2D(x)}\xi(t), \quad (1)$$

where the dots above x denote time derivatives, m is the mass of the particle, $\gamma(x)$ is the friction coefficient, $D(x)$ is the diffusivity, and $\xi(t)$ is a Gaussian white noise that incorporates the stochasticity—equipped with ensemble-averaged mean $\langle \xi(t) \rangle = 0$ and correlation $\langle \xi(t)\xi(t') \rangle = \delta(t - t')$. The Langevin equation simplifies significantly in the overdamped regime, in which we are interested in a typical observation time τ_o much larger than the inertial timescale of the particle, i.e. $\tau_o \gg m/\gamma$. In this regime, we have the overdamped Langevin equation,

$$\dot{x}(t) = \sqrt{2D(x)}\xi(t), \quad (2)$$

from which the statistics of the particle’s dynamics are determined solely by the diffusivity $D(x)$.

Discretisation conventions — To simulate a particle trajectory, one can iteratively integrate Eq. (2) in small timesteps Δt ,

$$x(t + \Delta t) = x(t) + \int_t^{t+\Delta t} ds \sqrt{2D(x(s))}\xi(s), \quad (3)$$

which presents a choice when it comes to evaluating the integral on the right-hand side of Eq. (3). Specifically, the diffusivity is a function of position, which is a random variable. To perform the numerical integration, one must choose which value the random variable takes in the interval $[x(t), x(t + \Delta t)]$ in order to evaluate the diffusivity. However, there is no uniquely determined point at which it *should* be evaluated. Instead, the choice is a matter of the adopted convention, which is parameterised by the continuous variable $\alpha \in [0, 1]$ in the following [20],

$$x(t + \Delta t) = x(t) + \sqrt{2D[(1 - \alpha)x(t) + \alpha x(t + \Delta t)]} \int_t^{t+\Delta t} ds \xi(s), \quad (4)$$

where the integral $\int_t^{t+\Delta t} ds \xi(s)$ is numerically evaluated by drawing a random number from a zero-mean Gaussian distribution of variance Δt .

Three common conventions are Itô ($\alpha = 0$) [17], Stratonovich ($\alpha = 1/2$) [18], and isothermal/Hänggi-Klimontovich ($\alpha = 1$) [21, 22], the latter of which we will refer to as “anti-Itô”. Each convention has its merits, which have been discussed at length in other works [14, 20, 23]. However, any $\alpha > 0$ essentially requires evaluating the diffusivity at a future timestep. The most direct route to simulating $\alpha > 0$ is thus to reformulate the dynamics in terms of the non-anticipatory Itô convention, $\alpha = 0$, either through a correction term [20] or an auxiliary step [24, 25]—see SM Sec. SII. Importantly, the chosen convention affects the statistics of the particle’s dynamics. This is elucidated by the Fokker-Planck equation, which describes the time evolution of the particle density,

$$\frac{\partial P(x, t)}{\partial t} = \frac{\partial}{\partial x} D^\alpha(x) \frac{\partial}{\partial x} D^{1-\alpha}(x) P(x, t). \quad (5)$$

The Fokker-Planck equation is distinct from a heat equation by having a corresponding Langevin equation that directly describes the evolution of the individual particle positions. However, given its similarity to the Fokker-Planck equation, we will use prior results for the heat equation to inform our derivation of the spatially varying diffusivity that achieves particle cloaking [7, 8]. The derived diffusivity will then be used to simulate an ensemble of diffusive particles by time-evolving their positions through the two-dimensional counterpart to the discretised Langevin equation (4), i.e.

$$x_i(t + \Delta t) = x_i(t) + g_{ij}[(1 - \alpha)\mathbf{x}(t) + \alpha\mathbf{x}(t + \Delta t)] \int_t^{t+\Delta t} ds \xi_j(s), \quad (6)$$

where $i, j \in \{1, 2\}$ enumerate the components of vectors (such as the position $\mathbf{x} = (x_1, x_2)$ and noise $\boldsymbol{\xi} = (\xi_1, \xi_2)$), as well as matrices—such as the square root of the diffusivity/diffusion tensor $\mathbf{g} = \sqrt{2\mathbf{D}} = ((g_{11}, g_{21})^T, (g_{12}, g_{22})^T)$. Above and throughout, a repeated index implies summation over that index.

Transformed Fokker-Planck equation — The general strategy to derive the properties of the cloak begins with performing a coordinate transformation that maps the protected region to a different region, see Fig. 1. Here, the protected region will be a circular core of radius R_1 that will be mapped to a surrounding annulus $R_1 \leq r' \leq R_2$, where r' is the radial distance from the origin in the new coordinates. This annular region acts as the cloak, with the specific space-dependence of the diffusivity in this region determined through the specific coordinate transformation, see below.

First, we consider the effect of a general coordinate transformation $\mathbf{x} \rightarrow \mathbf{x}'$ on the Fokker-Planck equation in two dimensions. Starting from the Fokker-Planck equa-

tion describing homogeneous diffusion of strength D_0 ,

$$\frac{\partial P(\mathbf{x}, t)}{\partial t} = \frac{\partial}{\partial x_i} D_0 \frac{\partial P(\mathbf{x}, t)}{\partial x_i}, \quad (7)$$

we want to find the (heterogeneous and anisotropic) diffusion tensor \mathbf{D}' in the new coordinate system that produces cloaking. Essentially, this requires manipulating the transformed Fokker-Planck equation into the same form as Eq. (7), whence identification of \mathbf{D}' in place of D_0 readily follows. Leaving the details to Sec. SI of the supplementary material (SM), we have for the Fokker-Planck equation after a general coordinate transformation [7],

$$\frac{\partial P(\mathbf{x}', t)}{\partial t} = \frac{1}{\det(\mathbf{J})} \frac{\partial}{\partial x'_j} J_{kj}^{-1} D_0 J_{kl}^{-1} \det(\mathbf{J}) \frac{\partial P(\mathbf{x}', t)}{\partial x'_l}, \quad (8)$$

where the components of the Jacobian matrix \mathbf{J} are given by $J_{ij} = \partial x'_j / \partial x_i$. Equation (8) poses the dynamics on an effective manifold [26], whereas we desire the coordinate transformation to leave the Fokker-Planck equation in an invariant ‘‘Euclidean’’ form analogous to Eq. (7). What prevents us from doing this is the space-dependent factor $1/\det(\mathbf{J})$ preceding the spatial derivatives. In the case of the heat equation, this factor is merely absorbed into the specific heat capacity [7, 8]. However, there is no analogous trick for the case of stochastic particle diffusion, since it depends solely on the spatially varying diffusivity $\mathbf{D}'(\mathbf{x})$. Hence, Eq. (8) is as far as one can go under a *general* coordinate transformation.

Non-linear transformation — The most-studied transformation is one where the radial distance from the centre of the protected region (and cloak) linearly transforms as $r' = R_1 + r(R_2 - R_1)/R_2$ for $r \leq R_2$ [6, 27, 28]. This has $\det(\mathbf{J}) = (R_2/(R_2 - R_1))^2 (r' - R_1)/r'$ for $r \leq R_2$, which is not constant and therefore motivates us to consider alternative transformations. As it turns out, finding a transformation that simultaneously maps the

protected region, $r' < R_1$, to the annulus, $R_1 \leq r' \leq R_2$, while maintaining constant $\det(\mathbf{J})$ is difficult. *Close* to satisfying both properties is the following non-linear transformation [29, 30],

$$r' = \begin{cases} \sqrt{\beta r^2 + R_1^2}, & r \leq R_2, \\ r, & r > R_2, \end{cases} \quad (9)$$

where $\beta = (R_2^2 - R_1^2)/R_2^2$ and the azimuthal coordinate θ is invariant, i.e. $\theta' = \theta$. For the numerical integration of the Langevin equation (6), it is more convenient to work in Cartesian coordinates $\mathbf{x}' = (x', y')$ rather than polars (r', θ') . In Cartesians, we have the following Jacobian for the non-linear transformation,

$$\begin{aligned} \mathbf{J} &= \frac{\partial(x, y)}{\partial(r, \theta)} \frac{\partial(r, \theta)}{\partial(r', \theta')} \frac{\partial(r', \theta')}{\partial(x', y')} \\ &= \begin{cases} \mathbf{R}(\theta') \text{diag} \left(\frac{r'}{r\beta}, \frac{r}{r'} \right) \mathbf{R}(-\theta'), & R_1 < r' \leq R_2, \\ \mathbf{1}, & r' > R_2, \end{cases} \end{aligned} \quad (10)$$

where $\mathbf{R}(\theta)$ and $\mathbf{1}$ are the 2×2 rotation and identity matrices, respectively. The Jacobian (10) has a piecewise-constant determinant,

$$\det(\mathbf{J}) = \begin{cases} \frac{1}{\beta}, & R_1 < r' \leq R_2, \\ 1, & r' > R_2, \end{cases} \quad (11)$$

suggesting Eq. (8) can be brought into the desired form (7) on a piecewise basis under the transformation (9) above. On this piecewise basis, the factors of $\det(\mathbf{J})$ in Eq. (8) cancel, allowing us to approximate the governing equation for the particle density by

$$\frac{\partial P(\mathbf{x}', t)}{\partial t} \approx \frac{\partial}{\partial x'_j} \mathbf{D}'_{jk} \frac{\partial P(\mathbf{x}', t)}{\partial x'_k}, \quad (12)$$

where we have identified the piecewise diffusion tensor,

$$\mathbf{D}' = D_0 \mathbf{J}^{-\text{T}} \mathbf{J}^{-1} = \begin{cases} D_0 \beta \mathbf{R}(\theta') \text{diag} \left(\frac{r'^2 - R_1^2}{r'^2}, \frac{r'^2}{r'^2 - R_1^2} \right) \mathbf{R}(-\theta'), & R_1 < r' \leq R_2, \\ D_0 \mathbf{1}, & r' > R_2, \end{cases} \quad (13)$$

from which we can recover homogeneous diffusion $\mathbf{D}' = D_0 \mathbf{1}$, as in Eq. (7), by setting $R_1 = 0$. Strictly speaking, Eq. (12) is an equality everywhere except at $r' = R_2$, where there is an additional divergent contribution arising from the sharp jump in $\det(\mathbf{J})$, Eq. (11). This was neglected by approximating the piecewise-constant $\det(\mathbf{J})$ as constant across *all* space. Hence, we naïvely expect the diffusion tensor in Eq. (13) to yield far-from-perfect cloaking. Furthermore, Eq. (12) has the appearance of a two-dimensional analogue to the one-dimensional Fokker-Planck equation (5) with $\alpha = 1$, naïvely suggesting the

anti-Itô convention [21, 22] of the Langevin equation (6) would yield the best cloaking performance. However, such a prediction is based on the misguided presumption that the identification of α from Eq. (12) equally applies to Fokker-Planck equations other than just the one-dimensional case [20]. In fact, in higher dimensions, the correction term that arises when treating anti-Itô as a perturbation to Itô is generally not of the divergence form necessary to write the Fokker-Planck equation as a two-dimensional analogue of Eq. (5) [14]. As a result, we also trialed the diffusion tensor \mathbf{D}' , Eq. (13), in the

Langevin equation (6) for conventions other than just anti-Itô. This was further justified *a posteriori*, since we found the Itô convention [17] resulted in the best cloaking performance.

Simulation setup — We performed simulations to determine how well the cloak, with diffusivity given by Eq. (13), conceals the inner core. In these simulations, the core of radius R_1 is centred in a square box of linear size L . The box has periodic boundary conditions at the sides, $x' = -L/2$ and $x' = L/2$, a reflecting boundary at the top, $y' = L/2$, and an absorbing boundary at the bottom, $y' = -L/2$, such that all particles eventually leave the system through the absorbing boundary. A uniformly distributed line of N particles is initialised at the top of the box, $y' = L/2$, at time $t = 0$, i.e. $P(x', y'; t = 0) = \delta(y' - L/2) \sum_{i=1}^N \delta(x' + L/2 - iL/N)/N$. This setup is notably different to that of thermal cloaking, where the temperatures at the top and bottom of the box are kept fixed. Here, the setup is analogous to a single pulse of radiation emitted from the line $y' = L/2$ at $t = 0$. Strictly speaking, each particle contributes a Dirac delta function to the overall particle density $P(x', y'; t)$. However, for finite particle number N , we rather view the particle density in a coarse-grained sense, i.e. envisage the simulation box as being divided up into small cells of linear length ℓ , such that the density at a position (x, y) located in a particular cell is well approximated by $n/(N\ell^2)$, where n is the number of particles contained in that cell. In this sense, the true particle density $P(x', y'; t)$ is recovered in the thermodynamic limit $N \rightarrow \infty$, while considering smaller and smaller cells, i.e. $\ell \rightarrow 0$.

After initialisation, the particles diffuse around the simulation box according to Eq. (6) with a diffusion tensor given by Eq. (13)—see SM Sec. SIII for full details. In case particles penetrated the inner core $r' \leq R_1$, we chose the inner core to have the same homogeneous diffusivity D_0 as the medium surrounding the cloak. If the diffusion tensor results in perfect cloaking, then particles will be unable to penetrate the inner core, $r' \leq R_1$, and the particle density outside the cloak, $r' > R_2$, will match that of a simulation box containing no core at all times t . In other words, any observer measuring the density at a radius $r' > R_2$ would be unable to detect the presence of the inner core *and* the cloak because the density would be the same as in their absence. How closely these densities match gives a measure of the effectiveness of the cloak. To formally quantify this, one can measure the cumulative arrival distribution $\Pi(x, t_f)$ of particles at the absorbing boundary, which is analogous to a “splitting probability” commonly used to probe the first-passage properties of stochastic processes [13],

$$\Pi(x'; t_f) = \int_0^{t_f} dt D_0 \left. \frac{\partial P(x', y'; t)}{\partial y'} \right|_{y'=-L/2}, \quad (14)$$

where $D_0 \partial_y P(x', y'; t)$ is the particle current at position $\mathbf{x}' = (x', y')$ in the negative- y' direction. Equation (14) is

the density of particles that have arrived at a position x' on the absorbing boundary by time t_f . The spatial average of the arrival distribution asymptotically approaches unity as $t_f \rightarrow \infty$, i.e. $\lim_{t_f \rightarrow \infty} \int_{-L/2}^{L/2} dx' \Pi(x'; t_f)/L = 1$, signifying the absorption of all particles. As for the particle density, the arrival distribution in the simulation of the cloaked core must match that of the simulation of no core (and no cloak) for the cloak to be considered effective.

Simulation results — We performed the simulations described above for the Itô ($\alpha = 0$) [17], Stratonovich ($\alpha = 1/2$) [18], and anti-Itô ($\alpha = 1$) [21, 22] conventions of interpreting the Langevin equation (6). We found the Stratonovich and anti-Itô conventions resulted in poorer cloaking than that of Itô, signified by: particles penetrating the inner core; particles experiencing spurious large jumps near $r' = R_1$; and noticeable differences in the arrival distributions, Eq. (14), compared to that of no core. This is not surprising given that the application of the anti-Itô and Stratonovich conventions (even numerically) to physical scenarios involving “problematic” boundaries—such as the jump discontinuity at $r' = R_2$ and singularity at $r' = R_1$ in the diffusivity, Eq. (13)—is often ill-posed [14, 31–33]. Because of their poorer performance compared to Itô, we will omit further discussion of the results for the Stratonovich and anti-Itô conventions.

The key result of this work is that, remarkably, the Itô convention exhibited near-perfect cloaking signified by no particle penetration of the inner core and a cumulative arrival distribution, Eq. (14), that closely matched that of no core for all times t , see Fig. 2. “Near perfect” is to caveat a small discrepancy in the total number of particles that have been absorbed up to time t between the simulations of the cloaked core and no core. However, this is similar to behaviour seen for thermal cloaking, where there is typically a lapse in time before the cloaking becomes effective [34]. Moreover, this discrepancy all but disappears through some regularisation procedures that we introduce in SM Sec. SIII. Strikingly, the density of particles inside the cloak $R_1 < r' \leq R_2$ is markedly different to that seen for thermal cloaking, which typically sees a smooth radial decay in density from outside the cloak $r' > R_2$ to the inner cloak boundary $r' = R_1$ [7]. Here, there is a distinct “halo” of high particle density in the cloak to accommodate those particles that would otherwise be found in the inner core $r' < R_1$. This also suggests why the smooth radial decay in density for thermal cloaking must come at the price of penetration of the inner core [7].

Discussion and conclusion — Inspired by results for optical and thermal cloaking [6, 7], we demonstrated cloaking of a region of space from an ensemble of stochastically diffusing particles. This is in spite of the lack of form-invariance of the Fokker-Planck equation under a general coordinate transformation, as well as the inherent difficulties introduced by stochasticity. Our setup consisted of a circular core that we attempted to con-

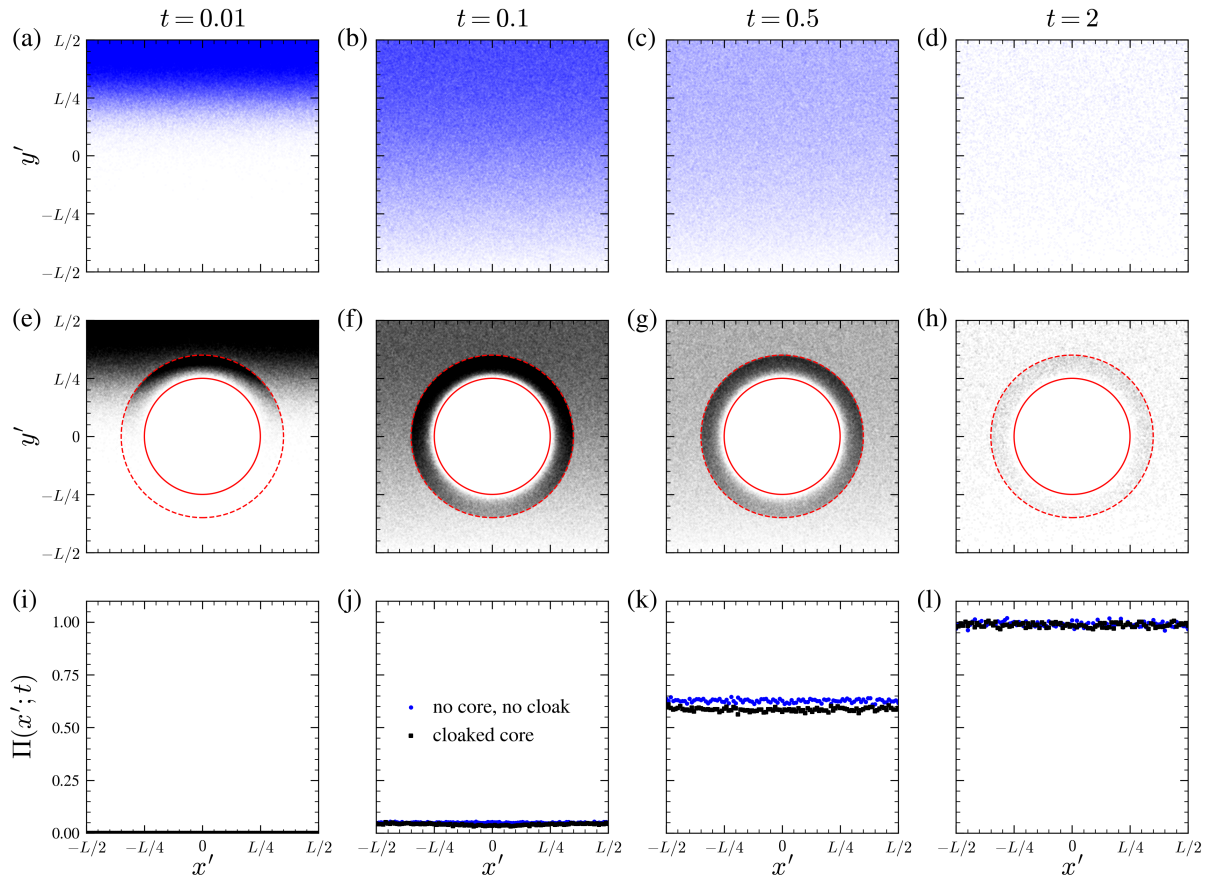


FIG. 2. Comparison between simulations of no core (a)–(d), and a cloaked core (e)–(h), with their corresponding cumulative arrival distributions $\Pi(x'; t)$, Eq. (14), (i)–(l) at times $t = 0.01$ in (a), (e), and (i); $t = 0.1$ in (b), (f), and (j); $t = 0.5$ in (c), (g), and (k); and $t = 2$ in (d), (h), and (l). Each data point in (a)–(h) represents the position of one of $N = 10^6$ particles. The simulation parameters used in all subfigures were $\Delta t = 10^{-5}$, $L = 1$, $D_0 = 1$. In (e)–(h), the inner core has radius $R_1 = 0.25$ (solid red line) and is surrounded by an annular cloak of outer radius $R_2 = 0.35$ (dashed red line). Particles are prevented from penetrating the core by the cloak in (e)–(h), and the cumulative arrival distributions $\Pi(x'; t)$ in (i)–(l) show that of the cloaked core closely matches that of no core for all times t , suggesting the diffusion tensor, Eq. (13), used in the cloaking simulations produces near-perfect cloaking.

ceal from particles by surrounding it with an annular metamaterial of spatially varying diffusivity. To quantify the degree of cloaking, we devised the “cumulative arrival distribution”, Eq. (14), which measured the spatial distribution of particles arriving along a tangential line downstream of the cloak. The hallmark of cloaking in this case is an arrival distribution that matches that of a simulation involving no core for all times. Our key result is a demonstration of near-perfect cloaking for the diffusion tensor D' in Eq. (13) if the Langevin equation is interpreted under the Itô convention [17], see Fig. 2. The cloaking performance can be further improved through two different regularisation procedures discussed in SM Sec. SIII. While we demonstrated near-perfect cloaking, the specific coordinate transformation we considered resulted in invariance of the Fokker-Planck equation only

on a piecewise basis. Therefore, future work should focus on establishing a firmer theoretical basis for the cloaking that results from the Itô convention. Another interesting avenue for further research would be to test stochastic cloaking on other cloak geometries, such as diamonds [35]. We believe this work has laid the foundations for a novel class of cloaking, thereby providing a completely new way to explore this intriguing phenomenon.

ACKNOWLEDGMENTS

C.R. acknowledges support from the Engineering and Physical Sciences Research Council (Grant No. 2478322). C.E. and H.R. acknowledge support from the Government of Spain (Ministerio de Ciencia e Innovación) through Project PID2021-125871NB-I00.

-
- [1] R. A. Shelby, D. R. Smith, and S. Schultz, *Science* **292**, 77 (2001).
- [2] D. R. Smith, W. J. Padilla, D. Vier, S. C. Nemat-Nasser, and S. Schultz, *Phys. Rev. Lett.* **84**, 4184 (2000).
- [3] A. Greenleaf, Y. Kurylev, M. Lassas, and G. Uhlmann, *SIAM Rev.* **51**, 3 (2009).
- [4] U. Leonhardt, *Science* **312**, 1777 (2006).
- [5] A. Ward and J. B. Pendry, *J. Mod. Opt.* **43**, 773 (1996).
- [6] J. B. Pendry, D. Schurig, and D. R. Smith, *Science* **312**, 1780 (2006).
- [7] S. Guenneau, C. Amra, and D. Veynante, *Opt. Exp.* **20**, 8207 (2012).
- [8] R. Schittny, M. Kadic, S. Guenneau, and M. Wegener, *Phys. Rev. Lett.* **110**, 195901 (2013).
- [9] M. Raza, Y. Liu, E. H. Lee, and Y. Ma, *J. Opt.* **18**, 044002 (2016).
- [10] S. A. Cummer and D. Schurig, *New J. Phys.* **9**, 45 (2007).
- [11] G. W. Milton, M. Briane, and J. R. Willis, *New J. Phys.* **8**, 248 (2006).
- [12] N. G. Van Kampen, *J. Stat. Phys.* **24**, 175 (1981).
- [13] N. G. Van Kampen, *Stochastic processes in physics and chemistry*, Vol. 1 (Elsevier, 1992).
- [14] C. Escudero and H. Rojas, arXiv:2309.03654 (2023).
- [15] R. Yuan and P. Ao, *J. Stat. Mech. Theory Exp.* **2012**, P07010 (2012).
- [16] R. Mannella and P. V. McClintock, *FNL* **11**, 1240010 (2012).
- [17] K. Itô, *Proc. Imp. Acad. Japan* **20**, 519 (1944).
- [18] R. L. Stratonovich, *SIAM J. Control* **4**, 362 (1966).
- [19] A. Pacheco-Pozo, M. Balcerak, A. Wyłomanska, K. Burnecki, I. M. Sokolov, and D. Krapf, *Phys. Rev. Lett.* **133**, 067102 (2024).
- [20] A. W. Lau and T. C. Lubensky, *Phys. Rev. E* **76**, 011123 (2007).
- [21] P. Hänggi, *Helv. Phys. Acta* **51**, 183 (1978).
- [22] Y. L. Klimontovich, *Phys.-Usp* **37**, 737 (1994).
- [23] I. M. Sokolov, *Chem. Phys.* **375**, 359 (2010).
- [24] R. Perez-Carrasco and J. Sancho, *Phys. Rev. E* **81**, 032104 (2010).
- [25] F. Sagués, J. M. Sancho, and J. García-Ojalvo, *Rev. Mod. Phys.* **79**, 829 (2007).
- [26] E. P. Hsu, *Stochastic analysis on manifolds*, 38 (American Mathematical Soc., 2002).
- [27] A. Greenleaf, M. Lassas, and G. Uhlmann, *Physiol. Meas.* **24**, 413 (2003).
- [28] A. Greenleaf, M. Lassas, and G. Uhlmann, *Math. Res. Lett.* **10**, 685 (2003).
- [29] C.-W. Qiu, L. Hu, B. Zhang, B.-I. Wu, S. G. Johnson, and J. D. Joannopoulos, *Opt. Exp.* **17**, 13467 (2009).
- [30] S. Guenneau, A. Diatta, T. M. Puvirajesinghe, and M. Farhat, *J. Opt* **19**, 103002 (2017).
- [31] Á. Correales and C. Escudero, *J. Math. Phys.* **60** (2019).
- [32] C. Escudero, *Stud. Appl. Math.* **145**, 719 (2020).
- [33] C. Escudero, *Phys. Scr.* **98**, 055214 (2023).
- [34] R. V. Craster, S. Guenneau, H. Hutridurga, and G. A. Pavliotis, *Multiscale Model. Sim.* **16**, 1146 (2018).
- [35] W. Li, J. Guan, Z. Sun, W. Wang, and Q. Zhang, *Opt. Exp.* **17**, 23410 (2009).
- [36] S. Bo and A. Celani, *Phys. Rep.* **670**, 1 (2017).
- [37] R. V. Kohn, H. Shen, M. S. Vogelius, and M. I. Weinstein, *Inv. Prob.* **24**, 015016 (2008).

SUPPLEMENTARY MATERIAL

SI. COORDINATE TRANSFORMATION OF THE FOKKER-PLANCK EQUATION

In this supplementary section, we derive Eq. (8), i.e. the result of applying a coordinate transformation to the Fokker-Planck equation (7) describing homogeneous diffusion of strength D_0 . For convenience, we repeat the latter here,

$$\frac{\partial P(\mathbf{x}, t)}{\partial t} = \frac{\partial}{\partial x_i} D_0 \frac{\partial P(\mathbf{x}, t)}{\partial x_i}, \quad (\text{S1})$$

where, as in the main text, a repeated index implies summation over that index.

The standard way [7] to proceed is to integrate Eq. (S1) against a scalar “test function” $\phi(\mathbf{x})$, where $\mathbf{x} = (x_1, x_2)$, whose properties are arbitrary aside from being infinitely differentiable and having compact support on the region $\Omega(\mathbf{x}) = [-L/2, L/2] \times [-L/2, L/2]$ in which the particles reside. From integrating Eq. (S1), we obtain

$$\int_{\Omega(\mathbf{x})} dx_1 dx_2 \frac{\partial P(\mathbf{x}, t)}{\partial t} \phi(\mathbf{x}) = - \int_{\Omega(\mathbf{x})} dx_1 dx_2 \frac{\partial \phi(\mathbf{x})}{\partial x_i} D_0 \frac{\partial P(\mathbf{x}, t)}{\partial x_i}, \quad (\text{S2})$$

where the boundary term from the integration by parts on the right-hand side vanishes due to the compact support property of $\phi(\mathbf{x})$.

Now, we consider the effect of a general coordinate transformation $\mathbf{x} = (x_1, x_2) \rightarrow \mathbf{x}' = (x'_1, x'_2)$. Under the change of coordinates, all instances of ∂_{x_j} in Eq. (S2) are replaced with $J_{ij}^{-1} \partial_{x'_j}$, where $J_{ij} = \partial_{x'_j} x_i$ are elements of the Jacobian matrix \mathbf{J} , and $dx_1 dx_2 = \det(\mathbf{J}) dx'_1 dx'_2$, i.e.

$$\int_{\Omega(\mathbf{x}')} dx'_1 dx'_2 \det(\mathbf{J}) \frac{\partial P(\mathbf{x}', t)}{\partial t} \phi(\mathbf{x}') = - \int_{\Omega(\mathbf{x}')} dx'_1 dx'_2 J_{ji}^{-1} \frac{\partial \phi(\mathbf{x}')}{\partial x'_i} D_0 J_{jk}^{-1} \det(\mathbf{J}) \frac{\partial P(\mathbf{x}', t)}{\partial x'_k}. \quad (\text{S3})$$

The integrand on the right-hand side of Eq. (S3) is merely the scalar product of the two vectors $\partial_{x'_i} \phi(\mathbf{x}')$ and $J_{ji}^{-1} D_0 J_{jk}^{-1} \det(\mathbf{J}) \partial_{x'_k} P(\mathbf{x}', t)$. Hence, upon another integration by parts to return the derivative $\partial_{x'_j}$ acting on the former to acting on the latter, followed by some rearrangement, we find

$$\int_{\Omega(\mathbf{x}')} dx'_1 dx'_2 \phi(\mathbf{x}') \left(\det(\mathbf{J}) \frac{\partial P(\mathbf{x}', t)}{\partial t} - \frac{\partial}{\partial x'_i} J_{ji}^{-1} D_0 J_{jk}^{-1} \det(\mathbf{J}) \frac{\partial P(\mathbf{x}', t)}{\partial x'_k} \right) = 0, \quad (\text{S4})$$

where the boundary term resulting from the integration by parts once again vanishes. It follows that if $P(\mathbf{x}', t)$ satisfies Eq. (S4) for an arbitrary test function $\phi(\mathbf{x}')$, then it also satisfies Eq. (8).

SII. SIMULATIONS OF DIFFERENT DISCRETISATION CONVENTIONS OF THE LANGEVIN EQUATION

Here, we detail how the simulations of the different discretisation conventions of the Langevin equation were performed. As discussed in the main text, the most direct route to simulating the $\alpha > 0$ cases is by reformulating the numerical integration of the Langevin equation (6) in terms of the non-anticipatory Itô convention [17], $\alpha = 0$, either through a correction term [20] or an auxiliary step [24, 25]. The correction term that arises when treating the other conventions as a perturbation to Itô typically involves spatial derivatives of the diffusion tensor \mathbf{D}' . Since the diffusion tensor here, Eq. (13), has a jump discontinuity at $r' = R_1$, this makes it difficult to simulate the dynamics through the correction-term approach. Thus, we instead opt for the auxiliary-step approach, which is able to handle discontinuities [24]. Qualitatively, this approach involves first generating an auxiliary position $\tilde{\mathbf{x}}(t + \Delta t)$ at the future timestep under the Itô convention. This auxiliary position is then interpreted as the “future” timestep at which to evaluate the diffusion tensor for an $\alpha > 0$ simulation, but still treating the Langevin equation (6) under the Itô convention. This correctly recovers the statistics of an $\alpha > 0$ simulation [24, 25]. More explicitly, the simulations are implemented by the following pseudocode, where all positions are to be understood as those in the new coordinates *after* applying the coordinate transformation:

initialise:

- Set particle index: $n = 1$;

while $n \leq N$ **do**

initialise:

- Set initial conditions: $t = 0$, $y(0) = L/2$, $x(0) = nL/N - L/2$;

while $t < t_f$ and $y(t) > -L/2$ **do**

- Generate two independent random numbers, $\mathcal{N}_1(0, \Delta t)$ and $\mathcal{N}_2(0, \Delta t)$, drawn from a Gaussian distribution of mean 0 and variance Δt , i.e. a distribution $G(x) = \exp(-x^2/(2\Delta t))/\sqrt{2\pi\Delta t}$;

- Calculate auxiliary “Itô” position:

$$\tilde{x}_I(t + \Delta t) = x(t) + g_{11}[\mathbf{x}(t)]\mathcal{N}_1(0, \Delta t) + g_{12}[\mathbf{x}(t)]\mathcal{N}_2(0, \Delta t);$$

$$\tilde{y}_I(t + \Delta t) = y(t) + g_{21}[\mathbf{x}(t)]\mathcal{N}_1(0, \Delta t) + g_{22}[\mathbf{x}(t)]\mathcal{N}_2(0, \Delta t);$$

- Calculate α -dependent position:

if $0 < \alpha \leq 1$ **then**

$$x(t + \Delta t) = x(t) + g_{11}[(1 - \alpha)\mathbf{x}(t) + \alpha\tilde{x}_I(t + \Delta t)]\mathcal{N}_1(0, \Delta t) + g_{12}[(1 - \alpha)\mathbf{x}(t) + \alpha\tilde{x}_I(t + \Delta t)]\mathcal{N}_2(0, \Delta t);$$

$$y(t + \Delta t) = y(t) + g_{21}[(1 - \alpha)\mathbf{x}(t) + \alpha\tilde{x}_I(t + \Delta t)]\mathcal{N}_1(0, \Delta t) + g_{22}[(1 - \alpha)\mathbf{x}(t) + \alpha\tilde{x}_I(t + \Delta t)]\mathcal{N}_2(0, \Delta t);$$

end

else

if $\alpha = 0$ **then**

$$x(t + \Delta t) = \tilde{x}_I(t + \Delta t);$$

$$y(t + \Delta t) = \tilde{y}_I(t + \Delta t);$$

end

end

- Implement periodic boundary conditions:

if $x(t + \Delta t) \geq L/2$ **then**

- $x(t + \Delta t) = x(t + \Delta t) - L$;

end

if $x(t + \Delta t) < L/2$ **then**

- $x(t + \Delta t) = x(t + \Delta t) + L$;

end

- Implement reflecting boundary condition:

if $y(t + \Delta t) > L/2$ **then**

- $y(t + \Delta t) = L - y(t + \Delta t)$;

end

- Increment time: $t = t + \Delta t$;

end

- Increment particle number: $n = n + 1$;

end

where t_f is the final time that the simulation is run to for each particle, Δt is the simulation timestep, N is the total number of particles, and g_{ij} are the elements of the matrix $\mathbf{g} = \sqrt{2\mathbf{D}}$, as in the main text, where \mathbf{D} can represent either the singular diffusion tensor of Eq. (13), or the non-singular diffusion tensor of Eq. (S9), see SM Sec. SIII, depending on whichever diffusion tensor is being simulated.

SIII. REGULARISATION AND REALISTIC CLOAKS

To corroborate the findings in the main text of near-perfect cloaking under the Itô convention, Fig. 2, we also performed simulations for two cases of stochastic cloaking that could more feasibly be implemented in an experiment.

A. Underdamped dynamics

The first of these is for the more general underdamped dynamics described by the two-dimensional analogue of Eq. (1), i.e.

$$m\ddot{\mathbf{x}}(t) = -\gamma(\mathbf{x})\dot{\mathbf{x}} + \gamma(\mathbf{x})\mathbf{g}(\mathbf{x})\boldsymbol{\xi}(t), \quad (\text{S5})$$

where the symbols retain their same definitions as in the main text. Here, the sharp jumps in the diffusivity \mathbf{D}' , Eq. (13), are regularised by the particles having inertia. The results of the overdamped case in the main text can be recovered for the underdamped dynamics by taking particle mass $m \rightarrow 0$ for a spatially varying diffusivity but constant friction coefficient. This is consistent with the recipe to recover the Itô convention of an overdamped Langevin equation from a discretisation-independent underdamped Langevin equation [36]. A snapshot of the particle density and arrival

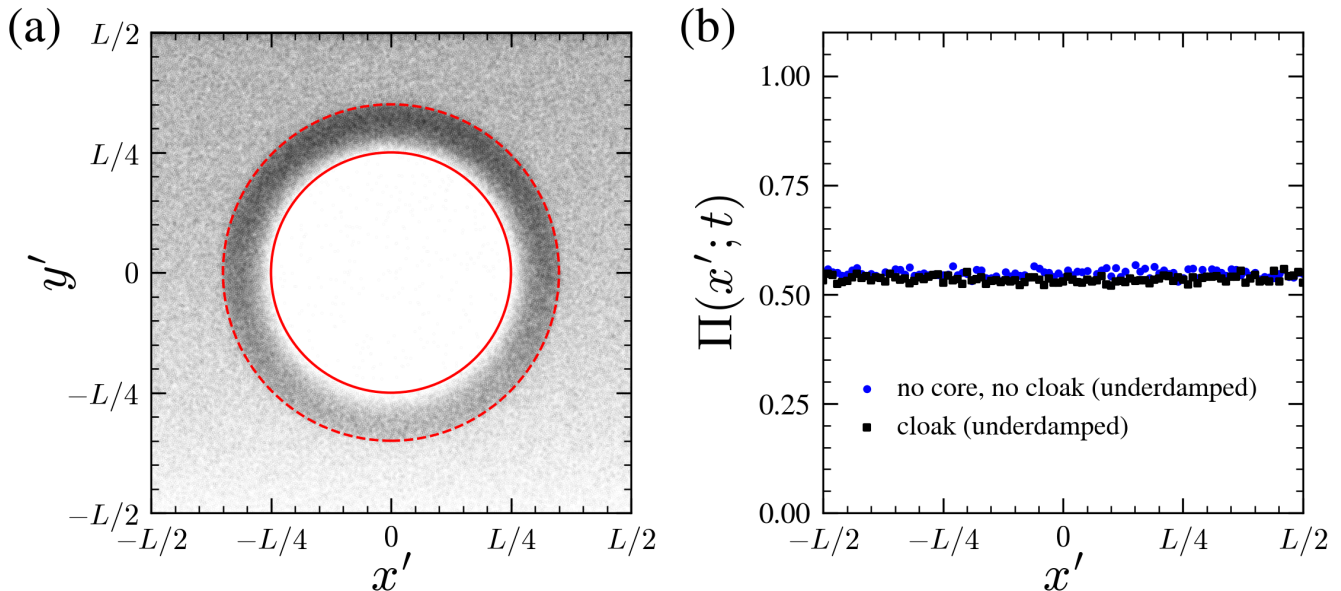


FIG. S1. (a) Snapshot at time $t = 0.5$ from a simulation of the underdamped dynamics described by Eq. (S5), for constant $\gamma = 1$ and using the diffusion tensor given in Eq. (13). Details of how the underdamped dynamics were simulated are given in Sec. SIII A. Each data point in (a) represents the position of one of $N = 10^6$ particles. (b) Corresponding cumulative arrival distribution $\Pi(x; t)$, Eq. (14), for the underdamped simulations of a cloaked core compared against that of no core. The simulation parameters used in both subfigures were $\Delta t = 10^{-5}$, $L = 1$, $D_0 = 1$, $m = 10^{-3}$, $R_1 = 0.25$, and $R_2 = 0.35$. We considered a small mass m such that the inertial timescale $m/\gamma \ll L^2/D_0$, thus making the dynamics close to the overdamped regime, illustrated in Fig. 2. However, the fact that there is a finite mass m is enough to regularise the singular behaviour of the diffusion tensor, Eq. (13), as evidenced by the cumulative arrival distribution $\Pi(x; t)$ for the cloaked core now more closely matching that of no core compared to the overdamped case. Furthermore, compared to the overdamped simulations illustrated in Fig. 2, less particles have been absorbed at $y' = -L/2$ up to time $t = 0.5$ because some particles “stick” to the reflecting boundary $y' = L/2$ for short periods of time due to their inertia. We also observe there to be some (albeit a very small amount of) particle penetration of the inner core in the underdamped case, which is the price paid for the regularisation provided by the finite mass m .

distribution from an underdamped simulation for constant $\gamma = 1$ (corresponding to $\alpha = 0$ in the overdamped regime) is illustrated in Fig. S1. As for the overdamped dynamics considered in the main text, Fig. 2, spatially varying γ (corresponding to $\alpha = 1$ in the overdamped regime) in the underdamped dynamics yet again produced relatively poor cloaking. For the finite but small m used in Fig. S1, the most notable difference to that of the overdamped dynamics, Fig. 2, is that the arrival distributions between the cloaked core and no core in the underdamped case agree more closely at all times than for the overdamped dynamics—though this comes at the price of some particle penetration of the inner core.

We now provide the pseudocode for the simulations of the underdamped Langevin equation (S5). By Einstein’s relation, diffusion D satisfies $\gamma D = k_B T$, where γ is the friction coefficient, k_B is the Boltzmann constant, and T is the temperature of the heat bath from which the diffusion derives. Hence, spatial modulation of the particle diffusivity can be achieved through either that of the friction γ or the temperature T . In the limit of particle mass $m \rightarrow 0$, the former corresponds to an anti-Itô convention [21, 22], $\alpha = 1$, of the overdamped Langevin equation (6), while the latter corresponds to that of an Itô convention [17], $\alpha = 0$ [36]. To allow a choice between the two, we implemented the underdamped dynamics through the following pseudocode:

initialise:

- Set particle index: $n = 1$;
- Choose $\alpha \in \{0, 1\}$;

while $n \leq N$ **do**

initialise:

- Set initial conditions: $t = 0$, $y(0) = L/2$, $x(0) = nL/N - L/2$, $v_x(0) = 0$, $v_y(0) = 0$;

while $t < t_f$ and $y(t) > -L/2$ **do**

- Generate two independent random numbers, $\mathcal{N}_1(0, \Delta t)$ and $\mathcal{N}_2(0, \Delta t)$, drawn from a Gaussian distribution of mean 0 and variance Δt , i.e. a distribution $G(x) = \exp(-x^2/(2\Delta t))/\sqrt{2\pi\Delta t}$;
- Update velocity according to the Langevin equation (S5):

if $\alpha = 1$ **then**

- Friction term is spatially varying, i.e.

$$v_x(t + \Delta t) =$$

$$v_x(t) + \frac{1}{m} [-v_x(t)\Delta t(D^{-1}[\mathbf{x}(t)])_{11} - v_y(t)\Delta t(D^{-1}[\mathbf{x}(t)])_{12} + 2(\mathbf{g}^{-1}[\mathbf{x}(t)])_{11}\mathcal{N}_1(0, \Delta t) + 2(\mathbf{g}^{-1}[\mathbf{x}(t)])_{12}\mathcal{N}_2(0, \Delta t)];$$

$$v_y(t + \Delta t) =$$

$$v_y(t) + \frac{1}{m} [-v_x(t)\Delta t(D^{-1}[\mathbf{x}(t)])_{21} - v_y(t)\Delta t(D^{-1}[\mathbf{x}(t)])_{22} + 2(\mathbf{g}^{-1}[\mathbf{x}(t)])_{21}\mathcal{N}_1(0, \Delta t) + 2(\mathbf{g}^{-1}[\mathbf{x}(t)])_{22}\mathcal{N}_2(0, \Delta t)];$$

end

else

if $\alpha = 0$ **then**

- Friction term is constant, i.e.

$$v_x(t + \Delta t) = v_x(t) + \frac{1}{m} [-v_x(t)\Delta t + g_{11}[\mathbf{x}(t)]\mathcal{N}_1(0, \Delta t) + g_{12}[\mathbf{x}(t)]\mathcal{N}_2(0, \Delta t)];$$

$$v_y(t + \Delta t) = v_y(t) + \frac{1}{m} [-v_y(t)\Delta t + g_{21}[\mathbf{x}(t)]\mathcal{N}_1(0, \Delta t) + g_{22}[\mathbf{x}(t)]\mathcal{N}_2(0, \Delta t)];$$

end

end

- Increment position:

$$x(t + \Delta t) = x(t) + v_x(t + \Delta t)\Delta t;$$

$$y(t + \Delta t) = y(t) + v_y(t + \Delta t)\Delta t;$$

- Implement periodic boundary conditions:

if $x(t + \Delta t) \geq L/2$ **then**

- $x(t + \Delta t) = x(t + \Delta t) - L$;

end

if $x(t + \Delta t) < L/2$ **then**

- $x(t + \Delta t) = x(t + \Delta t) + L$;

end

- Implement reflecting boundary condition:

if $y(t + \Delta t) > L/2$ **then**

- $y(t + \Delta t) = L - y(t + \Delta t)$;

end

- Increment time: $t = t + \Delta t$;

end

- Increment particle number: $n = n + 1$;

end

where, for simplicity, we set $k_B T = 1$ in the case of $\alpha = 1$, leading to $\gamma = \mathbf{D}^{-1}$, and set $\gamma = k_B = 1$ in the case of $\alpha = 0$, leading to $\mathbf{D} = T$. As in Sec. SII, t_f is the final time that the simulation is run to for each particle, Δt is the simulation timestep, N is the total number of particles, and g_{ij} are the elements of the matrix $\mathbf{g} = \sqrt{2\mathbf{D}}$.

B. A non-singular non-linear diffusion tensor

The second case we consider is to directly regularise the diffusion tensor \mathbf{D}' in Eq. (13), which is singular at the cloak's inner boundary $r' = R_1$. This singularity resulted from the implicit blowing up of an infinitesimally small ‘‘puncture’’ in the original coordinates to a finite region (circular core of radius R_1) under the coordinate transformation, see Fig. 1. This can be regularised from instead starting from a finite region of radius ϵ in the original coordinates [37], given by the following coordinate transformation,

$$r' = \begin{cases} \frac{R_1}{\epsilon} r, & r \leq \epsilon, \\ \sqrt{\beta_\epsilon r^2 + \lambda_\epsilon}, & \epsilon < r \leq R_2, \\ r, & r > R_2, \end{cases} \quad (\text{S6})$$

where $\lambda_\epsilon = R_2^2(R_1^2 - \epsilon_2)/(R_2^2 - \epsilon^2)$, $\beta_\epsilon = (R_2^2 - R_1^2)/(R_2^2 - \epsilon^2)$, and the azimuthal coordinate is once again invariant under the coordinate transformation, i.e. $\theta' = \theta$. The transformation in Eq. (S6) maps a region of finite radius ϵ

to the inner core of radius R_1 , i.e. $r' = R_1$ when $r = \epsilon$. In the limit $\epsilon \rightarrow 0$, one recovers the singular non-linear transformation of Eq. (9), with the singular behaviour at $r = 0$ now more evident from Eq. (S6) when taking this limit.

As in the main text, we calculate the Jacobian for this transformation in Cartesian coordinates. This results in

$$\mathbf{J} = \frac{\partial(x, y)}{\partial(r, \theta)} \frac{\partial(r, \theta)}{\partial(r', \theta')} \frac{\partial(r', \theta')}{\partial(x', y')} = \begin{cases} \frac{\epsilon}{R_1} \mathbb{1}, & r' \leq R_1, \\ \mathbf{R}(\theta') \text{diag} \left(\frac{r'}{r\beta_\epsilon}, \frac{r}{r'} \right) \mathbf{R}(-\theta'), & R_1 < r' \leq R_2, \\ \mathbb{1}, & r' > R_2, \end{cases} \quad (\text{S7})$$

which has a piecewise-constant determinant given by

$$\det \mathbf{J} = \begin{cases} \frac{\epsilon^2}{R_1^2}, & r' \leq R_1, \\ \frac{1}{\beta_\epsilon}, & R_1 < r' \leq R_2, \\ 1, & r' > R_2. \end{cases} \quad (\text{S8})$$

By bringing the general expression for the coordinate transformation of the Fokker-Planck equation into a form analogous to Eq. (7) on a piecewise basis, as done for the singular case in the main text, one can identify the piecewise diffusion tensor for the non-singular transformation as

$$\mathbf{D}'_\epsilon = D_0 \mathbf{J}^{-\text{T}} \mathbf{J}^{-1} = \begin{cases} D_0 \frac{R_1^2}{\epsilon^2} \mathbb{1}, & r' \leq R_1, \\ D_0 \beta_\epsilon \mathbf{R}(\theta') \text{diag} \left(\frac{r'^2 - R_1^2}{r'^2}, \frac{r'^2}{r'^2 - R_1^2} \right) \mathbf{R}(-\theta'), & R_1 < r' \leq R_2, \\ D_0 \mathbb{1}, & r' > R_2. \end{cases} \quad (\text{S9})$$

This regularised diffusion tensor is more easily mimicked by a metamaterial in an experiment, but comes at the price of allowing particles to penetrate the protected region $r' \leq R_1$. However, if the core is of homogeneous diffusivity, then it is still possible to conceal it from an external observer. Specifically, *given* a core of homogeneous diffusivity that we wish to conceal, cloaking is achieved by tuning the parameter ϵ in the cloak's spatially varying diffusivity such that the value $D_0 R_1^2 / \epsilon^2$ matches that of the core's given diffusivity.

Figure S2 shows a snapshot of the particle density and arrival distribution in the case of the non-singular diffusion tensor, Eq. (S9), where particle positions evolve according to the overdamped Langevin equation (6) interpreted under the Itô convention [17], $\alpha = 0$. The density is indistinguishable outside the cloak from that of a simulation of no core, as indicated by the arrival distribution more closely matching that of no core than for the singular diffusion tensor, Eq. (13), presented in the main text, Fig. 2.

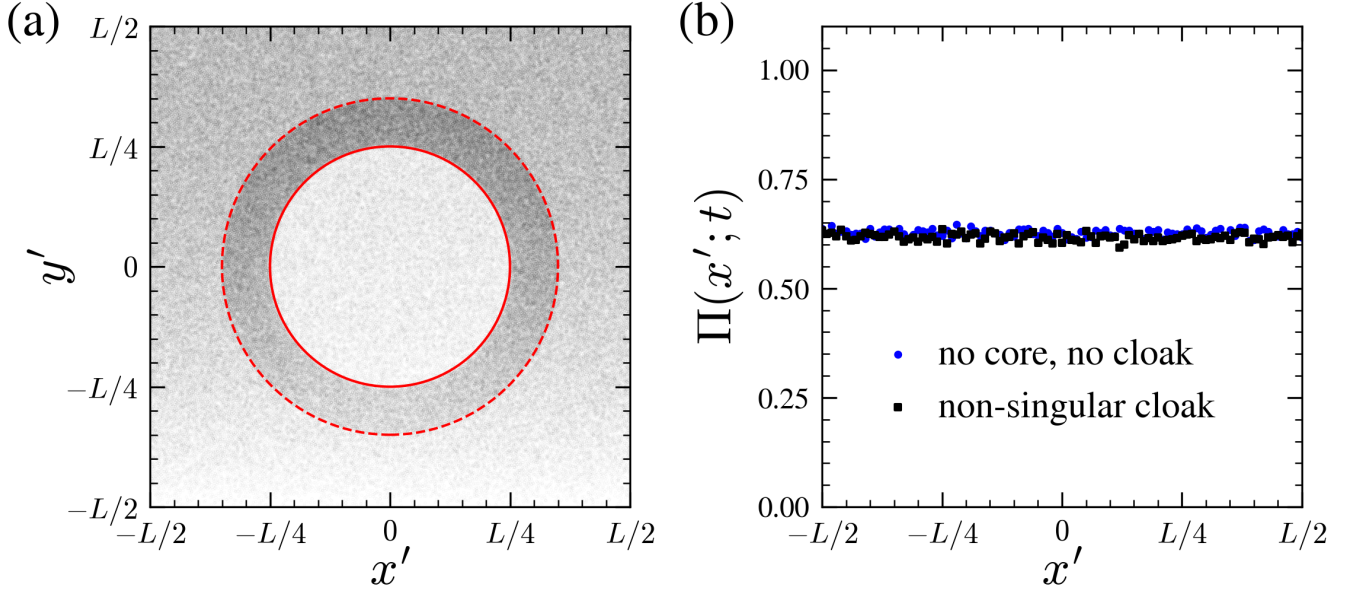


FIG. S2. (a) Snapshot at time $t = 0.5$ from a simulation using the non-singular diffusion tensor, Eq. (S9), derived in Sec. SIII B. Each data point in (a) represents the position of one of $N = 10^6$ particles. (b) Corresponding cumulative arrival distribution $\Pi(x; t)$, Eq. (14), for the simulations of the non-singular diffusion tensor compared against that of no core. The simulation parameters used in both subfigures were $\Delta t = 10^{-5}$, $L = 1$, $D_0 = 1$, $\epsilon = 0.2$, $R_1 = 0.25$, and $R_2 = 0.35$. Compared to the simulations of the singular diffusion tensor, Eq. (13), illustrated in Fig. 2, there is significant particle penetration of the inner core. However, if the core has a homogeneous diffusivity of $D_0 R_1^2 / \epsilon^2$, which is the case here, then the cumulative arrival distribution $\Pi(x; t)$ of the cloak better matches that of no core at all times, signifying that cloaking (in the sense that the particle density *outside* the cloak remains invariant) is achieved to a greater degree.